Mottl, M.J., Davis, E.E., Fisher, A.T., and Slack, J.F. (Eds.), 1994
Proceedings of the Ocean Drilling Program, Scientific Results, Vol. 139

36. STRUCTURE OF IGNEOUS BASEMENT AT SITES 857 AND 858 BASED ON LEG 139 DOWNHOLE LOGGING[1]

Marcus G. Langseth[2] and Keir Becker[3]

ABSTRACT

Ocean Drilling Program Leg 139 drilled at two sites located in an elongate zone of exceptionally high heat flow. Site 858 was located over an active vent field where heat flows exceeding 20W/m^2 have been measured. Site 857 was drilled 1.5 km to the south in an area where the local heat flow is about 1 W/m^2. Drilling and logging revealed strong contrasts in igneous basement structures and thermal regimes between the two sites. The lower 469 m of Hole 857D, which penetrated to a total depth of 936 m, consists of at least 27 distinct basaltic sills intercalated with turbidite sediments. Deep-sea drilling in Guaymas Basin, Yamato Basin, and now Middle Valley suggest that this layer-cake basement structure is typical of spreading centers located near copious sources of sediment. Temperatures are greater than 250°C at 500 mbsf at Site 857, but the temperature gradient to that depth is nearly uniform, suggesting that heat flow in the vertical direction is predominantly conductive. However, pore-water and sediment chemistry indicate lateral flow of pore water within the sediments. After Hole 857D was drilled into the sill-and-sediment complex, water flowed down the hole at an enormous rate and entered basement at two or more discrete and thin zones, one of which is believed to be associated with a normal fault.

Basalt was encountered at a shallower depth (258 mbsf) in Hole 858G. Logging and coring in the basaltic section indicate that basement below this site was constructed of extrusives. Seafloor heat flow, downhole temperature measurements, and open-hole temperature logs suggest the presence of a broad upwelling plume of high temperature water (≈280°C) comparable to that flowing from the vents. The results indicate that the active vent field is located over an extinct volcanic center which in the past may have stood as a small seamount above the floor of Middle Valley. Correlation of logs taken at Sites 857 and 858 sets constraints on the magmatic and tectonic evolution of the area encompassing the two sites.

INTRODUCTION

A primary objective of Ocean Drilling Program Leg 139 was to understand the subseafloor geometry of the hydrothermal system in Middle Valley, at the northern end of the actively spreading Juan de Fuca Ridge. Extensive geothermal and seismic exploration of the southern end of Middle Valley has produced a comprehensive map of seafloor heat flow and subseafloor structure that indicates areas of likely discharge, recharge, and active venting of high-temperature water (Davis and Villinger, 1992). The distribution of heat flow shows a rough inverse correlation with the depth to the base of the sedimentary layer, suggesting that temperatures in the underlying igneous units are fairly uniform, requiring that good hydrological communication be maintained by a relatively free lateral flow of hydrothermal fluids below the sediments (Davis and Lister, 1977). One of the objectives of Leg 139 drilling was to drill into this "hydrologic basement" to make direct measurements and obtain samples.

An initial concept of the hydrologic basement was that the upper igneous basement had a structure similar to that of Layer 2A at unsedimented mid-oceanic ridges; i.e., an extrusive carapace made up of pillow structures, sheet flows, and volcanoclastics. This layer is typically porous and permeable (Anderson and Zoback, 1982; Becker, 1989) and in typical oceanic settings appears to be an effective conduit for lateral subseafloor flow of pore fluids (Fisher et al., 1990, Langseth et al., 1992, Baker et al., 1991). However, this model may be too simple, for multichannel seismic reflection transects across Middle Valley reveal strong reverberant reflectors within and below the sediments. These reflectors are interpreted as basaltic sills (Rohr and Schmidt, this volume) that have intruded the sediments more or less parallel with bedding. These sills could have a profound effect on the geometry of fluid flow paths in the subseafloor.

The deepest penetration into basement was achieved at Sites 857 and 858, which were designed as complementary sites. At Site 858 an active vent field was drilled to examine a high-temperature discharge zone (Fig. 1). The seismic data indicates that this vent field sits over a local basement high, which probably stood as a small seamount above the seafloor in the past. Site 857 was drilled about 1.5 km to the south of the vent field. A seismic line across Site 857 (Fig. 2A) indicates that a layer of sediment about 500 m thick is underlain by sills. Trains of strong reflections below the uppermost sill suggest that there may be a series of sills interbedded with sediment deeper in the section (Davis and Villinger, 1992). The seismic reflections from horizons below the sill-and-sediment complex are masked, making it impossible to discern a reflector that might correspond to the top of an extrusive igneous basement analogous to Layer 2A at unsedimented ridges.

Drilling at Sites 857 and 858 yielded an enormous amount of new data on the nature of igneous structures in Middle Valley and their role in controlling the flow of fluid and heat. This paper describes logging results in the drill holes at these two sites, which provide evidence on the structure and constraints on the evolution of the igneous complexes in Middle Valley. Data relevant to logs that were successfully run at Sites 857 and 858 are listed in Table 1.

SILL-AND-SEDIMENT SEQUENCES AT SITE 857

Holes 857C and 857D penetrated a thick layer of sediment (≈465 m) overlying a sequence of sills and interbedded sediments. In Hole 857D the sill-and-sediment sequence was drilled to a depth of 936 mbsf without reaching a sediment-free igneous basement. In Hole 857C downhole logs were run through the sedimentary section and uppermost part of the sill-and-sediment sequence, and in Hole 857D the interbedded sill-and-sediment section was logged from 440 mbsf to the bottom of the hole.

Figure 3 shows logs of natural gamma and resistivity across the lowermost part of the sedimentary section and the top of the sill-and-

[1] Mottl, M.J., Davis, E.E., Fisher, A.T., and Slack, J.F. (Eds.), 1994. *Proc. ODP, Sci. Results*, 139: College Station, TX (Ocean Drilling Program).

[2] Lamont-Doherty Earth Observatory, Palisades, NY 10964, U.S.A.

[3] Division of Marine Geology and Geophysics, Rosenstiel School of Marine and Atmospheric Science, University of Miami, Miami, FL 33149, U.S.A.

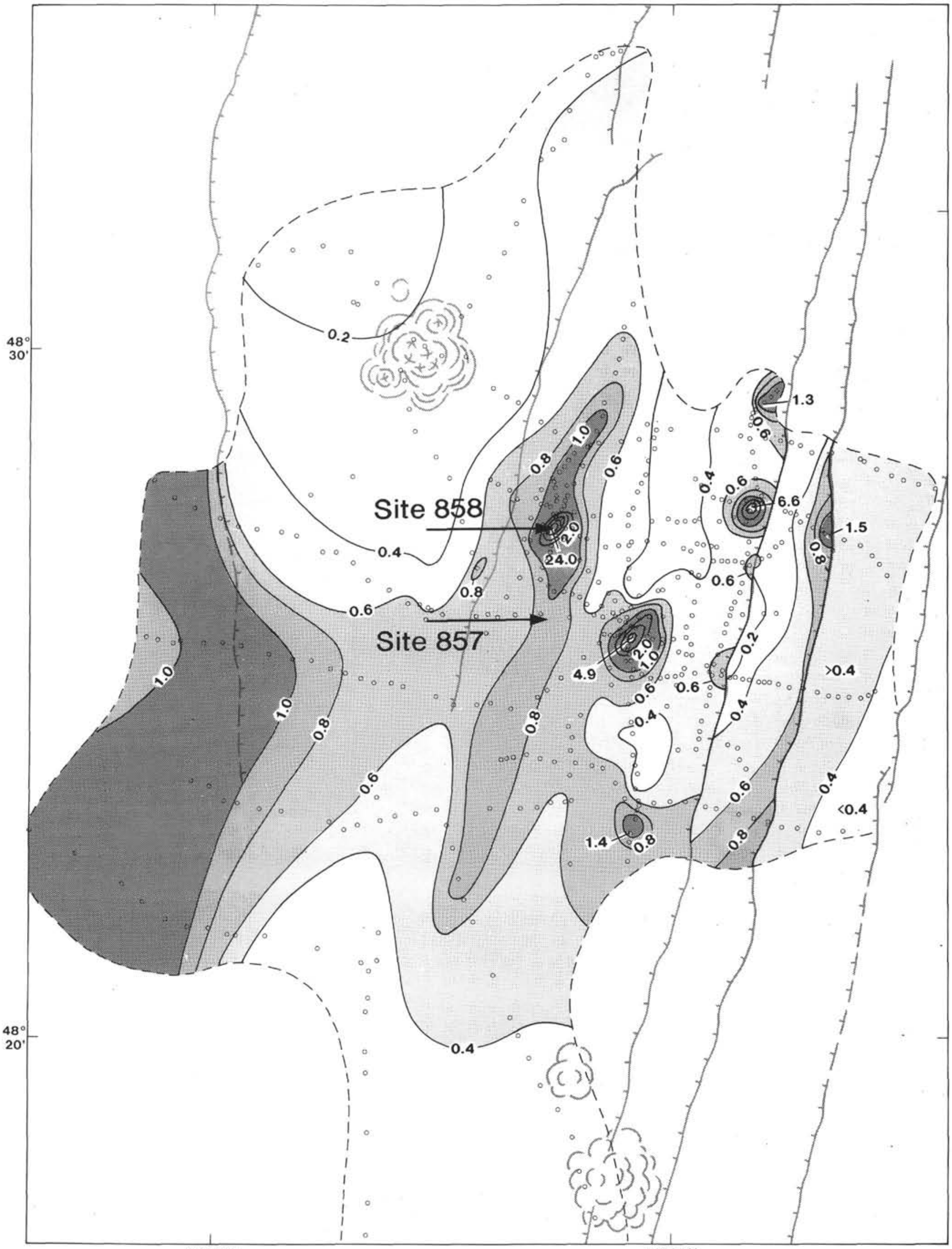

Figure 1. Contour map of heat flow in southern Middle Valley showing major normal faults and locations of Sites 857 and 858. From Davis and Villinger (1992).

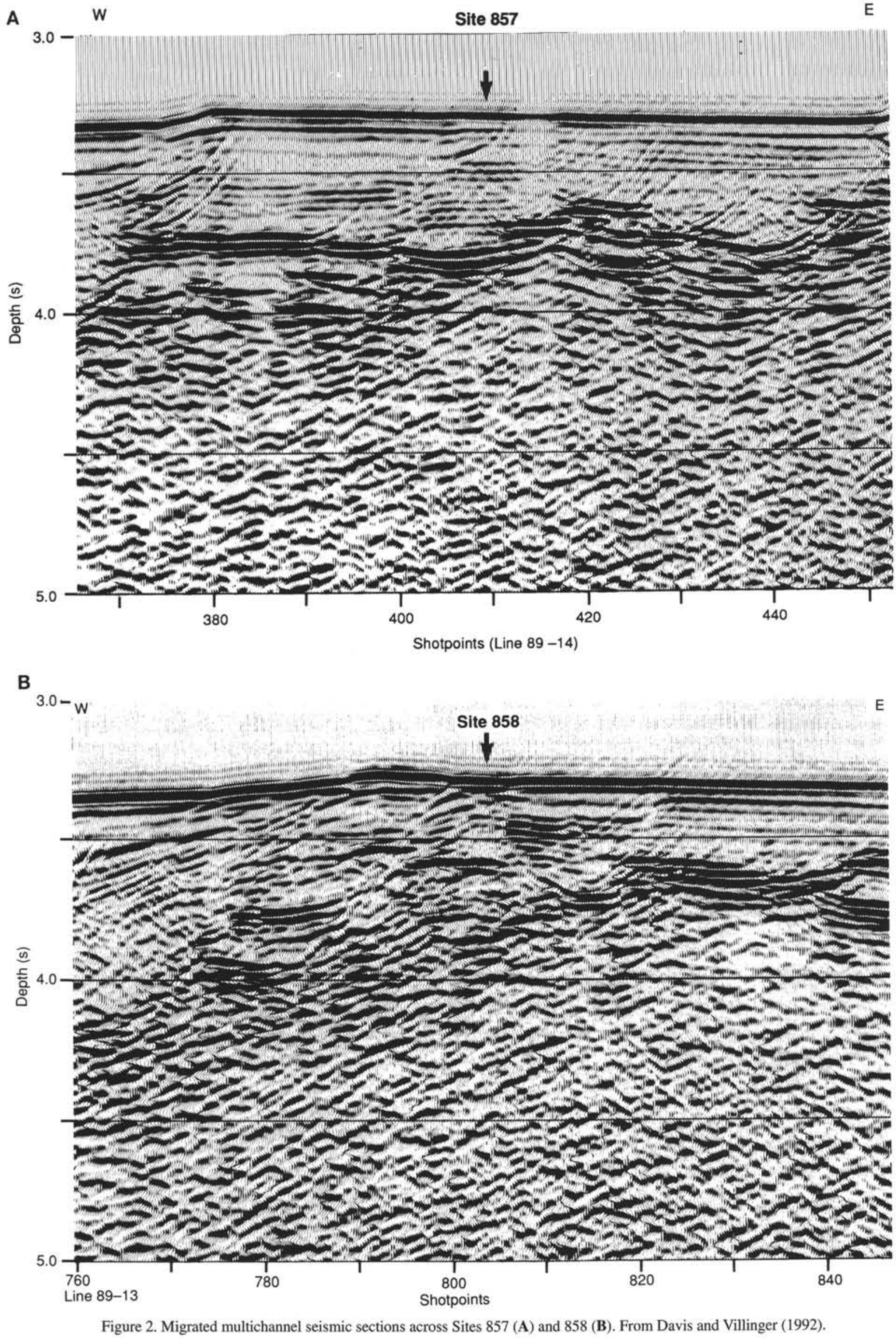

Figure 2. Migrated multichannel seismic sections across Sites 857 (**A**) and 858 (**B**). From Davis and Villinger (1992).

Table 1. Logging runs at Sites 857 and 858, Leg 139.

Hole/run number	Date/time (begin/end)	Tools[a]	Interval logged (mbsf)
HOLE 857C			
1	7/29 1347 7/29 1616	Self-recording high-temperature tool	Bottom-hole temp. 202 mbsf
2	7/30 0659 7/30 1010	Self-recording high-temperature tool	Bottom-hole temp. 288 mbsf
3	8/02 1428 8/02 2146	Sonic velocity/resistivity tools	129–541
4	8/03 0700 8/03 1300	Lithodensity/porosity tools	101–524
5	8/08 1010 8/08 1214	Self-recording high-temperature tool	107–193 mbsf
6	8/09 0146 8/09 0345	Self-recording high-temperature tool	272–321 mbsf
7	8/09 0607	Self-recording high-temperature tool	Bottom-hole temp. 476 mbsf
HOLE 857D			
1	8/23 1745 8/23 2248	Wireline high-temperature/pressure and flow tool	8–510
2	8/29 1049 8/29 1428	Wireline high-temperature/pressure and flow tool	0–936 mbsf
3	8/30 0555 8/30 1250	Sonic velocity/resistivity tools	460–936
4	8/30 1405 8/30 2000	Formation Microscanner (2 passes)	574–936 mbsf 574–830
5	9/01 0443 9/01 0650	Lithodensity/porosity tools (2 passes)	565–750 565–662
HOLE 858A			
858A-1	8/12 1840 8/12 2240	Self-recording high-temperature tool	70–264
HOLE 858B			
858B-1	8/13 2209	Self-recording high-temperature tool	Bottom-hole temp. 37 mbsf
HOLE 858F			
1	8/18 0811 8/19 0400	Self-recording high-temperature tool	Bottom-hole temp. 264 mbsf[b]
2	8/18 1645 8/18 2200	Wireline high temperature pressure and flow tool	0–241
3	8/19 1245 8/19 1830	Sonic velocity/resistivity tools	28.6–299
4	8/19 2020 8/20 0200	Formation Microscanner	48–259.0
HOLE 858G			
1	9/3 0532 9/3 0840	Self-recording high-temperature tool	0–160-in casing
2	9/6 1052 9/6 1452	Self-recording high-temperature tool	0–379
3	9/7 0740 9/7 1400	Lithology density/porosity tools	241–348
4	9/7 1758 9/7 2200	Self-recording high-temperature tool	0–398

[a] The natural spectral gamma tool was run on all strings except the high-temperature tools.
[b] The GRC high-temperature tool accidently free fell to the bottom of the hole and was fished out about 19 hr later. The instrument still contained valid data and suffered only minor damage.

sediment sequence in Hole 857C. The natural gamma ray log discriminates well between sedimentary and basaltic rocks in the hole; sedimentary sections are characterized by relatively high counts of natural gamma radiation (20–40 API units), whereas in basaltic sections counts are an order of magnitude lower (2 to 3 API units). The resistivity log also clearly shows the location of basaltic sills as zones of higher resistivity. Velocity and density logs were also clear indicators of basaltic units.

The natural gamma log in the lower part of Hole 857D (440–920 m) shows that at least 26 individual basaltic sills were penetrated, with thicknesses varying from 1 m up to 25 m (Fig. 4). The sills have a combined thickness of approximately 190 m, or 41% of the drilled sequence. The noisy resistivity log for Hole 857D occurred because the ship experienced high amplitude heaving during logging operations with no heave compensation on the wireline. Nonetheless, the resistivity log shows the thicker sills as higher resistivity zones.

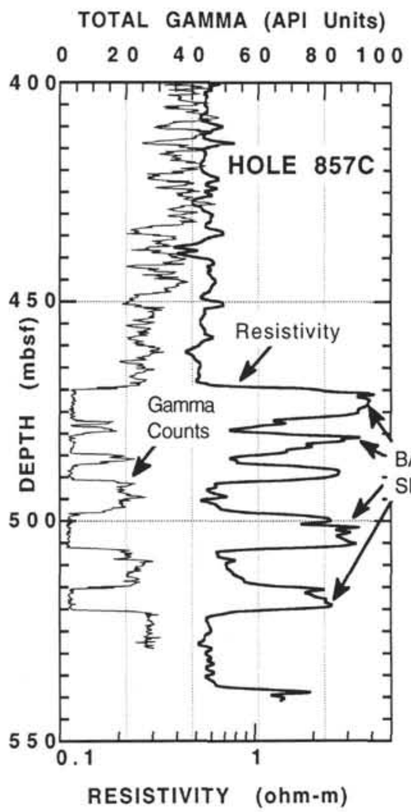

Figure 3. Total natural gamma ray counts and resistivity logs in the bottom 140 m of Hole 857C. The basaltic sections can be seen clearly as zones of low gamma ray counts and high resistivity.

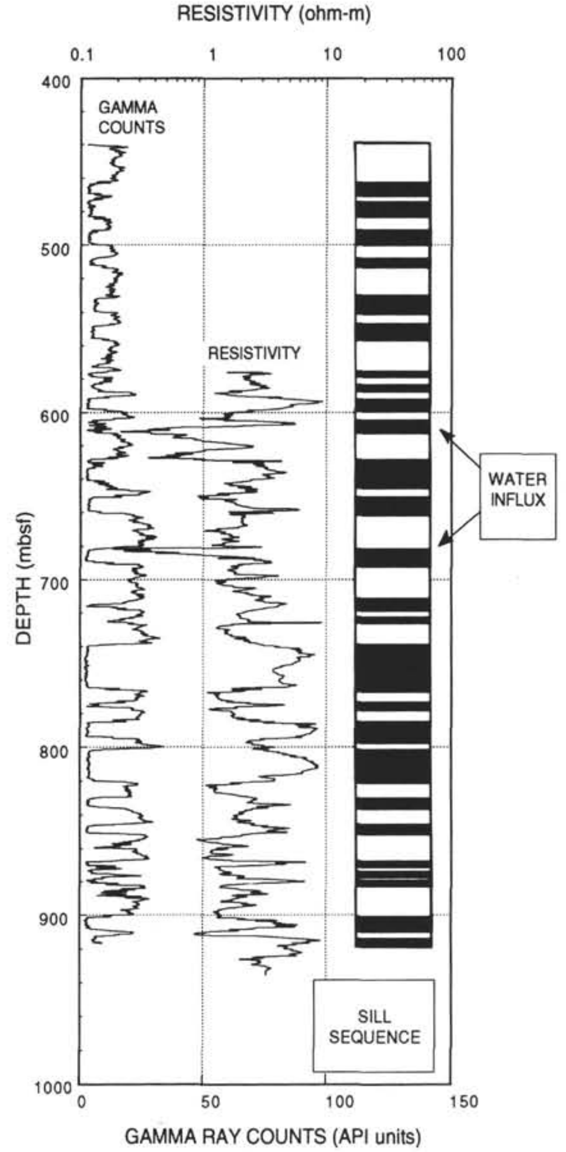

Figure 4. Total natural gamma ray counts and resistivity logs in the sill-and-sediment sequence in Hole 857D. Note that the gamma ray log also indicates the location of basaltic layers through the casing. The location of individual sills is shown as solid black bars in the strip on the right.

The assertion that the basaltic layers are sills as opposed to flows or dikes is based on three different lines of evidence: (1) Seismic sections across Middle Valley show that reverberant trains of reflectors associated with sill-and-sediment sequences are prevalent throughout Middle Valley, but no lava flows are currently exposed on the seafloor on top of the sediments (Davis and Fisher, this volume; Rohr and Schmidt, this volume); (2) samples of the upper contacts of the sills show baked sediments and highly altered and mineralized veins in the basalt (Shipboard Scientific Party, 1992a); and (3) Formation Microscanner Scanner (FMS) images in Hole 857D show that the sediments above contacts of the igneous units are deformed (Fig. 5A).

The FMS images in the sill-and-sediment sequences in Hole 857D and also at the top of the igneous units in Hole 858F (Figs. 5A and B) show pervasive fracturing of the igneous and sedimentary rocks. Many of the fractures have a vertical orientation and an azimuthal alignment with the trend of the spreading center and bounding faults. Some of the vertical fracturing may be drilling induced, most probably by thermal stresses created by circulating water with a temperature of a few tens of degrees into formations at temperatures greater than 250°C. The alignment of these fractures with the expected direction of maximum horizontal compressive stress and the observation that many of the vertical fractures continue into the sedimentary layers supports the possibility that they are thermal stress fractures. The fractures are quite ragged (Fig. 5), unlike fractures typically produced by circumferential stresses generated by drilling, suggesting that thermal stresses may have opened or produced connections between preexisting fractures.

Both the igneous and the sedimentary units are crisscrossed by wide fractures. The fractures in the igneous units are more prominent in the FMS images because of the greater contrast in resistivity between the fractures and the solid rock. If these fractures are not sealed by mineralization, the network of cracks should give the sill-and-sediment sequence a relatively high permeability.

The sediments in the sill-and-sediment sequence are compacted and no doubt strengthened by the heating and loading that accompanies the injection of the sills. This increase in consolidation is reflected in the velocities and densities measured on samples of the interbedded sediments (Shipboard Scientific Party, 1992a) and in an increase in average level of the resistivity (lower water content) of the interbedded sediments compared to the sediments that lie above the sill-and-sediment sequence (Figs. 3 and 4). Because of the strengthening of the sediment, it is likely that the complex evolved by the injection of new sills at the top of the sequence where lower-density, less-consolidated sediment offers less resistance to injection of magma.

Sill-and-sediment interbedded sequences also form the acoustic basement in the Yamato Basin, Japan Sea (Tamaki, Pisciotto, Allan, et al., 1990) and the Guaymas Basin (Curray, Moore, et al., 1982). In these basins rapid sedimentation also accompanies the magmatism

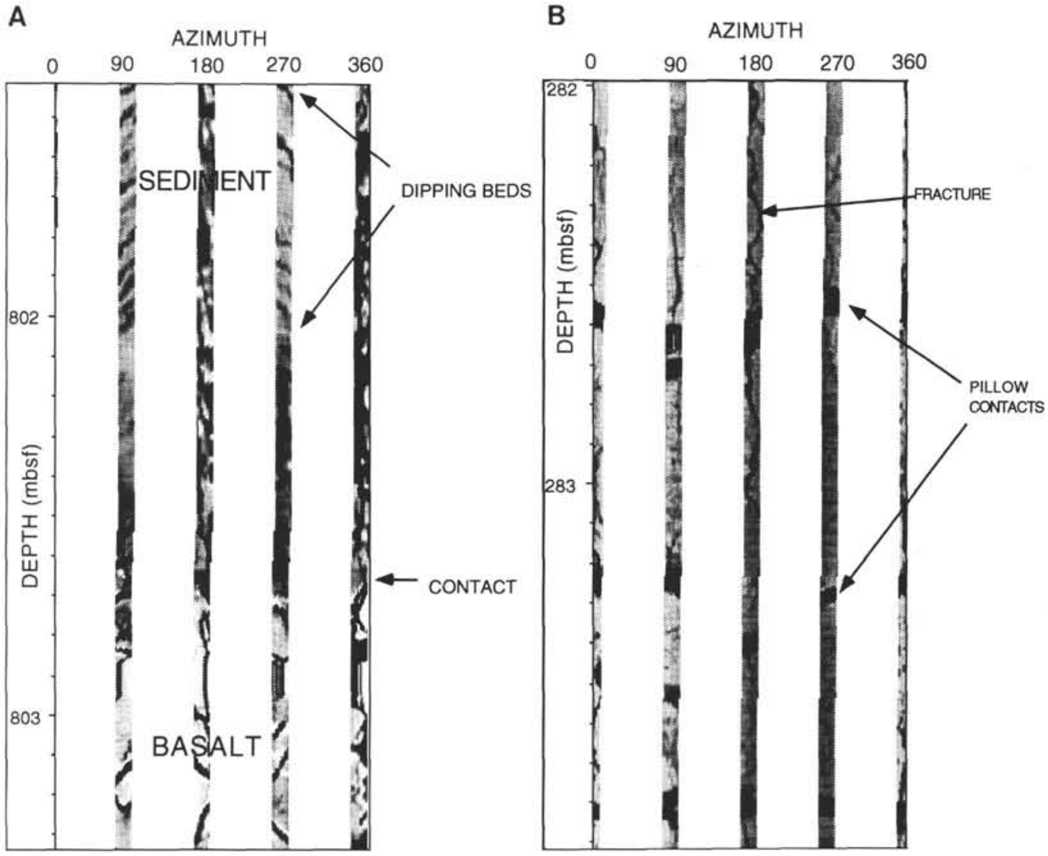

Figure 5. **A.** The FMS image of the upper contact of the largest sill drilled in Hole 857D with overlying sediment. Notice the ragged vertical fractures in both the basalt and sedimentary sections that are oriented roughly north-south (180° and 360°). **B.** The FMS image in the igneous section at the bottom of Hole 858F. The wide black bands running across the image are interpreted as clay-filled contacts between pillow units. The fine, nearly vertical fractures may be created by thermally induced stresses.

associated with spreading. The structure at Site 857 appears to be typical of basement where sediment is being deposited rapidly at a volcanically active spreading center, in strong contrast to unsedimented spreading centers, where the upper part of the oceanic basement is characterized by a more porous and possibly more permeable structure of pillow lavas, volcanoclastics, and flow sequences.

BASEMENT STRUCTURE AT SITE 858

Site 858 is located over an active vent field positioned over a small, buried seamount (Fig. 2B), which the seismic section shows as a small, dome-like edifice below the vent field. Gamma ray and resistivity logs run in the basement section of Holes 858F and 858G indicate much less sediment below the topmost igneous unit than was found at Site 857 (Fig. 6). The two low resistivity zones logged below 320 mbsf in Hole 858G may be associated with zones of high porosity where seawater is flowing into the rock surrounding the hole. The quality of the logs in this hole suffers from high amplitude heaving of the ship during logging; nevertheless, the resistivity is uniformly high and the natural gamma ray counts are uniformly low over much of the basement section. The FMS images in the upper part of basement in Hole 858F show pillow-like structures (Fig. 5B), and chilled margins were frequently noted in the core samples of basalt (Shipboard Scientific Party, 1992b). Thus, the upper 174 m of basement at Site 858 are not composed of interbedded sills and sediment as at Site 857. These results suggest that the basement high at Site 858 is a volcanic edifice constructed of flows and pillow lavas that probably stood as a small seamount above the seafloor before being buried by turbidites.

CORRELATION OF LOGS BETWEEN SITES AND CONSTRAINTS ON DEPOSITIONAL HISTORY

A strong correlation of the resistivity logs between Sites 858 and 857 over a 100-m interval in the sedimentary section supports the conjecture that basement at Site 858 is a buried seamount and provides evidence concerning the sequence of local magmatic, tectonic, and depositional events at the two sites. The resistivity logs from Holes 857C and 858F are compared in Figure 7. In Figure 7B the log at Hole 857C has been displaced upward about 50 m and compressed by about 10% to illustrate more clearly the correlation of resistivity peaks. The core samples from Holes 857C and 858F and FMS images in Hole 858F show that the high resistivity peaks are associated with thick turbidite deposits. Thus, the correlation is produced by a sequence of turbidites common to both sites. The correlation requires that during the time when turbidites were being deposited, the seafloor at both sites was at about the same elevation.

The resistivity logs shown in Figure 7A are in true depth relationship. A good correlation can be demonstrated only in the sections between 100 and 210 m in Hole 858F and 150–280 m in Hole 857C. Thus, the top of the correlative sequence at Site 857 is currently about 50 m deeper than at Site 858. At least three depositional or tectonic scenarios could result in this difference in depth: (1) the compaction of the thick layer of sediment below the correlative sequence at Site 857 was much greater than at Site 858 and led to a relative subsidence of the seafloor at Site 857 as deposition of sediments continued; (2) Sites 857 and 858 are located on the same tilted basement fault block and Site 857 is down dip from Site 858; tilting of the fault block as

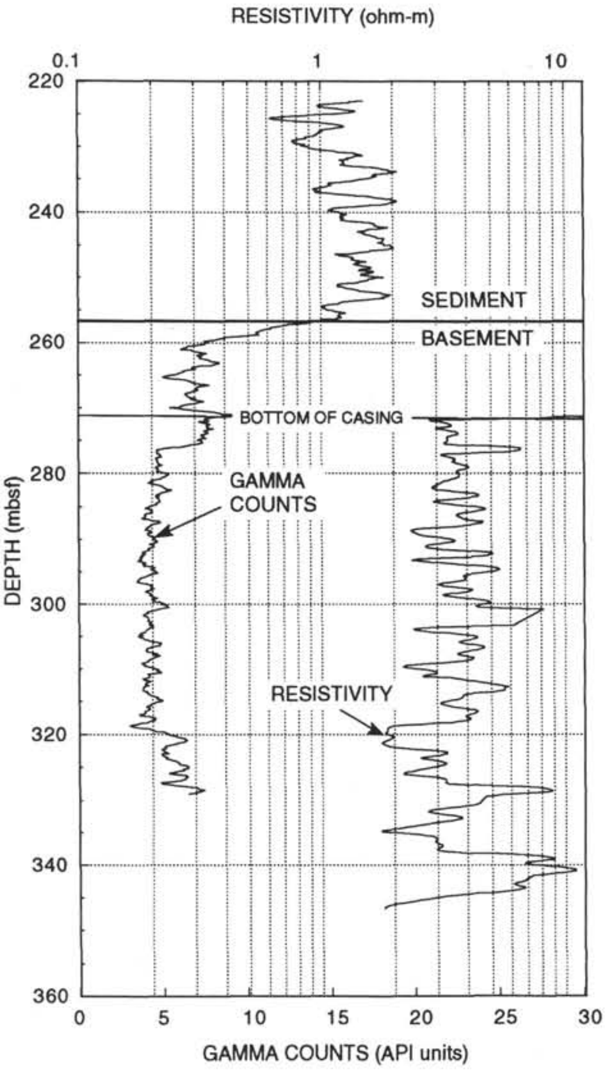

Figure 6. Natural gamma and resistivity logs in the bottom 120 m of Hole 858G. The upper 40 m are in the sediment that produces high gamma count, whereas the igneous units from 258 mbsf to the bottom of the hole show uniformly low counts. The low resistivity zones below 320 m are probably associated with high porosity zones where influx of cold seawater is occurring.

deposition of sediment continued led to fanning of the sequence with the thicker sequence building up at Site 857; and (3) relative movement on a normal fault between Sites 858 and 857 could explain the current greater depth of the correlative sequence.

Site 857 includes a 195-m-thick layer of sediment between the bottom of the correlative zone at 275 mbsf and the top of the first sill at 470 mbsf. In contrast, Site 858 has only a 48-m-thick layer of sediment between the bottom of the correlative zone at 210 mbsf and the top of the igneous units at 258 mbsf. This indicates that either the sedimentation rate at Site 858 was about four times lower than that at Site 857 when these sections were deposited, or that the duration of sediment deposition at Site 858 was shorter.

Evidence from coring and logging supports the first interpretation. Core recovery in the lower part of the sedimentary section in Hole 858F was typically only 1.5% to 3%. Nonetheless, the shipboard core descriptions record an abrupt change in the character of the sediment at 210 mbsf (bottom of the correlative sequence in Hole 858F). Above 210 mbsf the recovered sediments are predominantly coarse-grained siltstones and sandstones typical of deep-sea turbidite sequences,

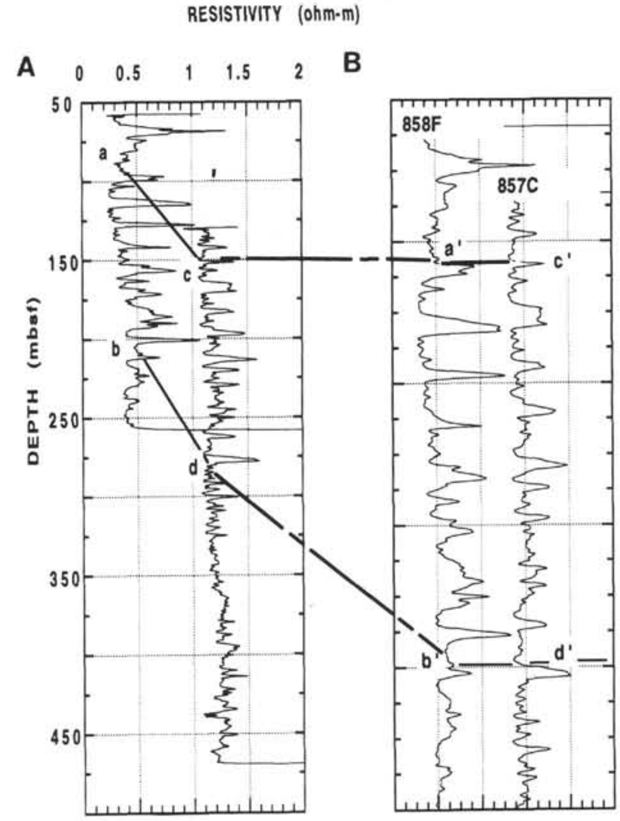

Figure 7. **A.** A comparison of the resistivity logs in Holes 857C and 858F. The trace corresponding to Hole 857C has been shifted 0.7 ohm-m to the right to avoid overlap. **B.** To better illustrate the correlation between the sites, the correlative sequence in Hole 857C is adjusted upward about 55 m and the scale compressed to 92% of original.

whereas the cores below 210 mbsf contain a "darker, softer, and fresher-looking" claystone (Shipboard Scientific Party, 1992b). In Hole 857C the sediments below the correlative section (>275 mbsf) continue to be sequences of thick turbidites with basal sandstones. We interpret this to mean that relatively finer sediments were being deposited hemipelagically at a slower rate on the summit of a volcanic edifice at Site 858, while coarser sediments were deposited on the surrounding seafloor. This suggests that the volcanic edifice below Site 858 stood above the seafloor as a small seamount at that time and received only the fine clayey components of the turbidity flows filling Middle Valley.

Figure 8 is a cartoon depicting a possible four-stage scenario in the magmatic, depositional, and tectonic development of the area containing Sites 857 and Sites 858, consistent with the logging and coring data. The scenario assumes that displacement of a normal fault caused the difference in depth of the correlative sequence described above.

SUMMARY OF DOWNHOLE TEMPERATURE OBSERVATIONS AT SITES 857 AND 858

Site 857

Seafloor heat-flow measurements and subseafloor temperature measurements at Site 857 indicate that the vertical heat transfer is predominantly conductive through the sedimentary section. A variety of subseafloor temperature measurements are shown in Fig. 9. Temperature measurements made with the water sampler and temperature probe (WSTP), which is inserted into sediment ahead of the drill bit during a pause in the drilling operations, give the best determination of

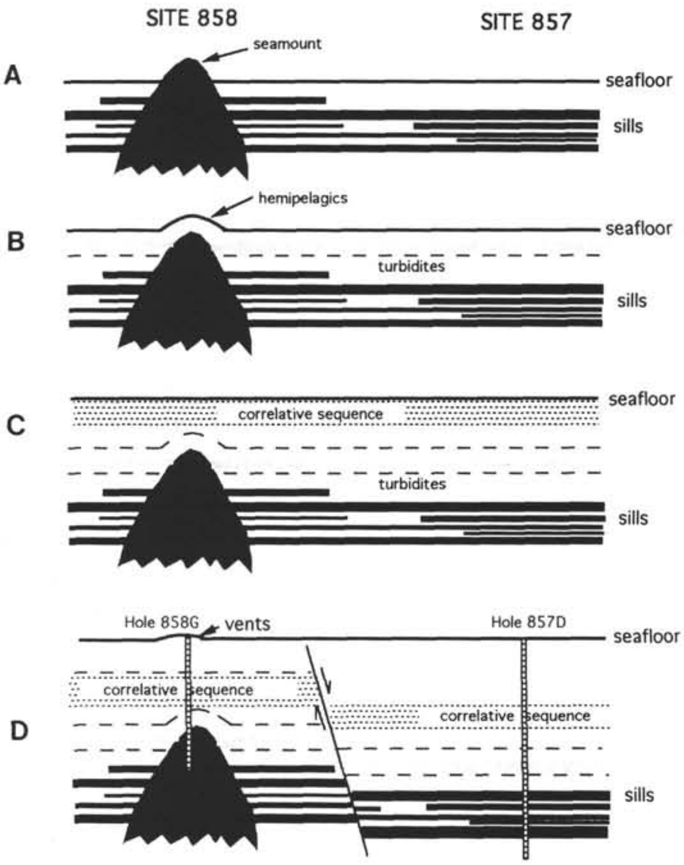

Figure 8. Cartoon showing possible evolution of the structures at Sites 857 and 858. **A.** The volcanic edifice that underlies Site 858 is formed by extrusive volcanism and projects above the seafloor. Turbidite deposition and possibly sill injection continue in surrounding deeper areas that include Site 857. **B.** Volcanism that formed the edifice stops and fine silts and clays are deposited over the summit of the seamount while turbidite deposition continues to bury surrounding areas at a much faster rate. **C.** Eventually the edifice and its hemipelagic drape are completely buried by sediments and subsequent turbidity flows cover both sites and form the 100-m-thick correlatable sequence observed by the logs. **D.** Lastly, the area around Site 857 subsides relative to the vent area, probably due to a combination of normal faulting and differential compaction.

the undisturbed formation temperatures (Shipboard Scientific Party, 1992a). WSTP measurements indicate a gradient of 71°C/km in Hole 857C, which we have used to estimate a conductive temperature profile to a depth of 500 m (dashed line in Fig. 9) using shipboard measurements of thermal conductivity. Extrapolations using conductivities predicted from porosities and corrected for the effects of temperature and anisotropy (see Davis and Wang, this volume; Davis and Seemann, this volume; Villinger et al., this volume) predicts temperatures of 250°C to 280°C at the top of the sill-and-sediment sequence. The other temperature measurements shown in Figure 9 were made in the open borehole during pauses in drilling. The Leg 139 *Initial Reports* volume (Davis, Mottl, Fisher, et al., 1992) contains more details about these measurements. All of the open-hole measurements fall below the predicted profile because the hole was still recovering from the effects of cold seawater circulated in the hole during drilling. Nonetheless, they support other evidence that the vertical heat transfer through the sedimentary section at Site 857 is primarily conductive.

Packer and flowmeter experiments in Hole 857D show evidence for a downward flow of water into the hole at rates of about 10,000 L/min (Becker et al., this volume). The profile of downward flow obtained by flowmeter measurements indicates that most of the water enters the formation in a discrete zone between 610 and 615 mbsf. The resistivity log in Hole 857D (Fig. 4) shows a large decrease in resistivity in the zone where this influx of water occurs. The spontaneous potential log also showed a large negative response in this zone (Shipboard Scientific Party, 1992a). The large decrease in resistivity indicates that the section of the hole where water is flowing into the formation at high rates is highly porous. Additional negative resistivity spikes at 630 and 685 mbsf indicate that there may be significant inflow of water at those levels as well. The spontaneous potential anomalies are believed to result from the chemical disequilibrium induced by the massive influx of cold seawater into the hot formation.

Temperature logs in Hole 857D that were made after completion of the hole clearly show the thermal effects of the rapid downflow of cold seawater (Fig. 10). The borehole above 610 mbsf is virtually isothermal as a result of the rapid downflow. An abrupt increase in temperature gradient at 610 mbsf suggests that most of the seawater enters the formation at that depth. Similar abrupt increases of gradient at 690 mbsf and 825 mbsf suggest that water may be entering the formation at those levels as well. Packer experiments indicate that the sill-and-sediment sequence below 736 mbsf has a permeability comparable to the upper few hundred meters of igneous oceanic crust measured elsewhere (Becker et al., this volume). The influx of water at high rates occurs only at a limited number of thin zones, which we believe are associated with major faults that intersect Hole 857D at 610–630 mbsf, 685–690 mbsf, and possibly at 825 mbsf.

Site 858

Subseafloor temperature measurements in the vent field area revealed extremely high temperatures (200°C) at shallow depths (20 mbsf), which is consistent with the high heat flow and the high-temperature water (≈280°C) issuing from the active vents. Such high temperatures at shallow depth must be supported by an upward flow of pore water from below. Rough estimates of vertical volumetric flow rate can be made based on a one-dimensional model that assumes upward flow of pore fluids. Assuming an average heat flow of about 12 W/m^2 over the vent field (Davis and Villinger, 1992), and an asymptotic temperature at depth of 280°C, the upward volumetric flow of pore water is estimated to be about 40 cm/yr. On the other hand, if it is assumed that the temperature increases to 95% of the asymptotic value in the upper 50 m as the data suggest, then the upward volumetric flow is estimated to be 65 cm/yr. Although this simple model is probably a significant departure from reality, it shows that relatively low volumetric flow rates can support high surface heat flows and seafloor gradients. Alternative models of the pattern of vertical flow through the sediments at Site 858 are described by Davis and Villinger (1992).

Temperature profiles in the open hole in Hole 858G (Fig. 11) provide additional important information relative to the hydrothermal regime. The temperature profile measured on September 3 was logged while the casing was plugged with cement at the bottom end. The plugged and water-filled casing had been left undisturbed for 11.5 days prior to logging. The temperature profile (shown by small open circles) indicates temperatures of 265°C at 40 mbsf, but deeper in the cased hole the temperature decreases, going through a minimum of about 105°C at 80 mbsf, and then increasing gradually with depth to about 250°C at 180 mbsf. The temperature minimum is believed to be an artifact created by the flow of cold water down Hole 858F, which is only 8–10 m away. The cold water flowing down Hole 858F apparently spread radially within the sedimentary strata, significantly cooling a zone between 50 and 200 mbsf. This requires that the sediment in this zone be relatively permeable compared to sediments in the upper 50 m because radial flow from Hole 858F in the upper 50 m of the section is apparently inhibited. The likely predrilling temperature profile is indicated by the smooth curve of fine dots in Figure 11. It is obvious that the pore water that spread laterally from Hole 858F absorbed a large amount of heat to reduce the formation temperatures by nearly 150°C.

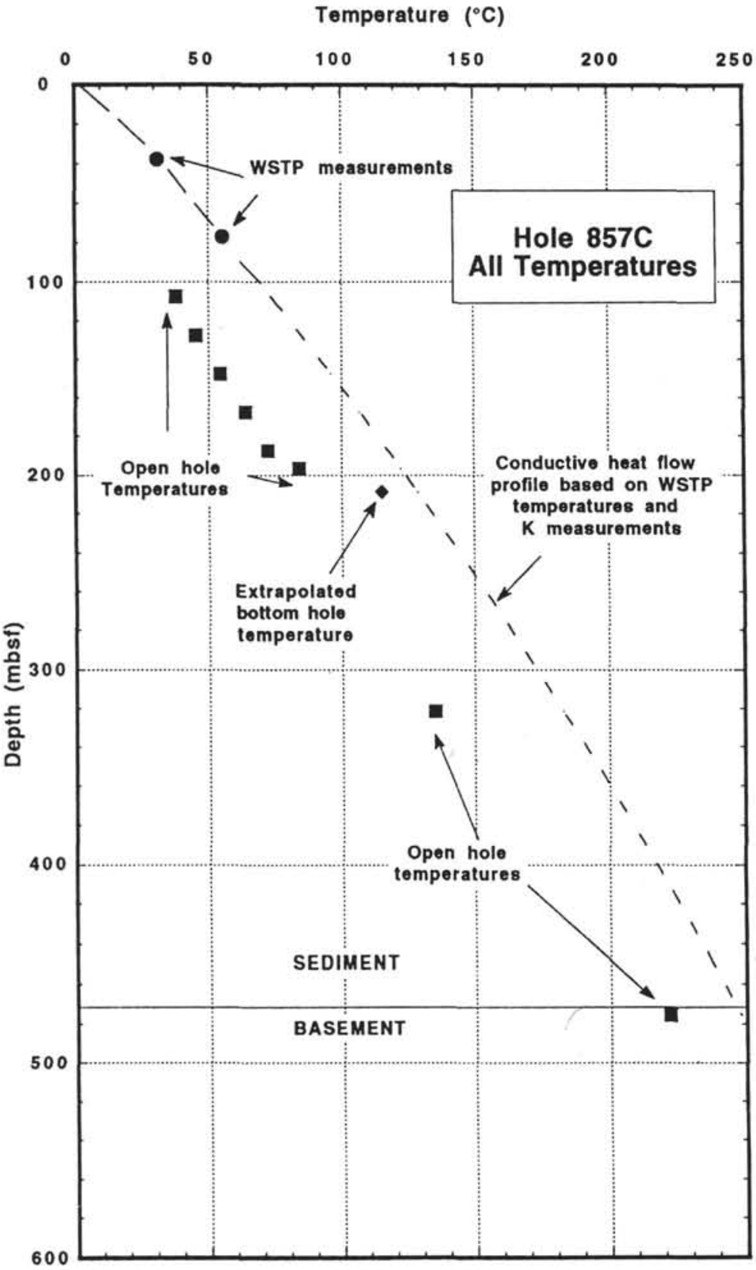

Figure 9. Temperature measurements in Hole 857C. Except for the WSTP measurements, all temperature points have been disturbed to some extent by drilling.

Two additional temperature profiles were measured after the hole was drilled to its full depth. The September 6 profile was made soon after drilling had been completed and the September 7 profile about 31 hours later. The low thermal gradient in the upper 330 m of the hole indicates flow of water down the hole that is driven by the difference between the cold hydrostatic pressure in the borehole and the hot hydrostatic pressure in the surrounding formation (about 0.8 MPa). A simple model of the heat exchange between the water flowing down the hole and the hole walls (Becker et al., 1983) provides an estimate of the flow of about 150 L/min, which is about two orders of magnitude less than the induced flow down Hole 857D. The sharp break in the gradient at about 330 mbsf suggests that as in Hole 857D, water enters the formation through a thin, discrete zone in the hole wall. However, there is no evidence for an extremely high permeability zone in the upper 174 m of the igneous units at Site 858 comparable to those at Site 857. Below 330 mbsf the increase in temperature gradient indicates that there is little or no flow below this level in the hole. Bottom-hole temperatures are increasing rapidly, as is seen by comparing the September 6 and 7 profiles (Fig. 11).

DISCUSSION

Relationship Between Basement Structures and the Flow of Hydrothermal Fluids

Drilling during Leg 139 did not directly detect or measure natural flow of pore fluids in the hydrothermal system in Middle Valley. The observations that were made yield indirect information on the distribution and intensity of flow. These observations include measurements of parameters such as in-situ pressures, temperatures, and pore-water chemistry, and relevant physical properties such as permeability, porosity, thermal conductivity, and density. Added to these measurements are the results of experiments that give estimates of hydraulic and thermal properties by artificially introducing pressure and thermal transi-

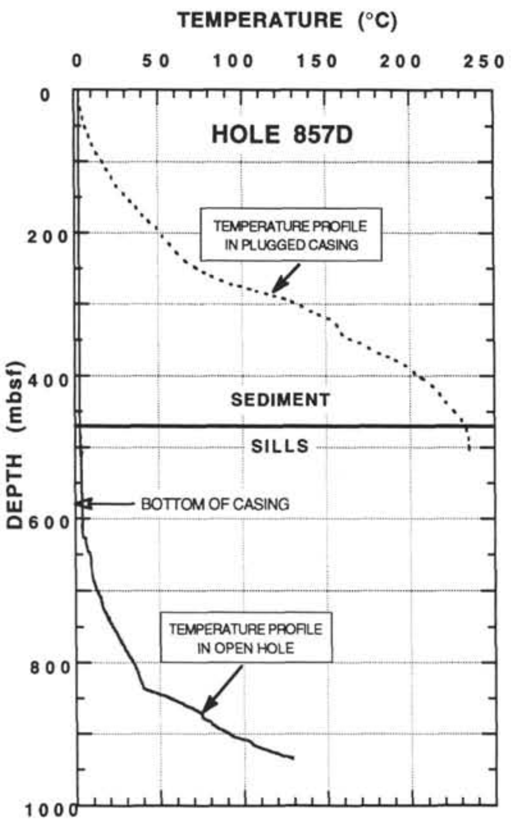

Figure 10. Two temperature profiles of Hole 857D, one made in the casing that was plugged at the bottom (dashed line) and the other made after the hole had been drilled to full depth. Notice that this profile is virtually isothermal from the seafloor to 610 mbsf. Abrupt breaks in gradient occur where water flows into the formation.

ents in the drill holes. Although the locations of holes drilled on Leg 139 were selected to sample important components of the hydrothermal system (areas of discharge and recharge), the holes represent only a few points in a vast and complex hydrothermal system. Consequently, the most important outcome of Leg 139 drilling will be the association of the observed parameters and properties with subseafloor lithologies and structures. These associations can be used to extend the fragmentary data gathered on Leg 139 to other areas of Middle Valley where the geology and structure has been imaged by geophysical techniques.

An important observation is that the structure of the crust at spreading centers that are rapidly inundated with sediments is distinctly different from the structure at unsedimented ridges. At sedimented spreading centers, sediments are incorporated into the igneous crust as it forms. Consequently, the upper igneous units are made up of sequences of sills and laccoliths that have intruded into the sedimentary section. Seismic data suggest that the intrusives in Middle Valley have their sources in fissure eruptions that parallel the spreading center (Rohr and Schmidt, this volume). In this environment it is unlikely that a 200- to 500-m-thick, highly porous and permeable layer is formed, comparable to Layer 2A at unsedimented ridges. The igneous units below the sill-and-sediment sequences are likely to be sheeted-dike complexes found in ophiolites and drilled in Hole 504B. We note that the permeability of the sheeted-dike complex at Hole 504B is three to four orders of magnitude lower than the upper extrusive layers of the crust (Becker, 1989). If there is a relatively free lateral flow of hot hydrothermal fluids in a "hydrologic basement" below the sedimentary layer, suggested by the seafloor heat flow data (Davis and Villinger, 1992), it would have to occur in a sill-and-sediment sequence.

Extensive fracturing of the sills and interbedded sediment is seen in the FMS images of the hole walls in the sill-and-sediment sequences, and should result in a relatively high fracture permeability. However, the packer experiments at Site 857 (Becker, this volume) indicate that the sill-and-sediment sequence below 756 mbsf has a permeability of about 2×10^{-14} m^2. The flowmeter data in Hole 857D and temperature logs suggest that seawater is flowing down the hole and entering basement through a few thin, high-permeability zones that intersect the hole. These zones are probably associated with normal faults and may serve as high-permeability conduits for the vertical and lateral flow (in the plane of the fault zone) of hydrothermal fluids. The elongate region of higher heat flow that was mapped just east of the complex of bounding faults (see Fig. 1) may be a reflection of the upward flow of water along highly fractured zones associated with normal faults. The conduits provided by the faults may not reach the seafloor due to the overlying low-permeability sediments (Fisher et al., this volume), but they may interconnect levels of horizontal flow within more permeable zones in the sedimentary section and the sill-and-sediment sequence.

It may be expected that the structure of the sill-and-sediment sequence will produce a pronounced anisotropy in the large-scale permeability. Vertical flow is probably inhibited by mineralization in fractures at the many contacts between igneous and sedimentary rocks, except where the sequence is cut by faults. The abundant fractures within the sills and interbedded sediments as revealed in the FMS images should provide a relatively high permeability path for horizontal flow in zones of limited thickness. The nearly uniform basement temperatures across Middle Valley that are indicated by downward extrapolation of seafloor heat-flow measurements to basement may result primarily from the ease with which pore fluids flow laterally in the sill-and-sediment sequence.

The efficient lateral subseafloor flow of pore fluids from Hole 858F to Hole 858G about 10 m away suggests that some sedimentary layers also have a relatively high permeability. At Site 858 a fracture permeability in the sediments may result from diagenesis induced by high temperatures at shallow depths below the vents and deeper in the sedimentary section throughout Middle Valley. Pervasive fracture permeability would add significantly to the permeability created by the sequences of coarse-grained turbidites and clay strata. Although uniform heat flow with depth in Hole 857C indicates that vertical heat transport through the sedimentary layer in Middle Valley is predominantly by conduction, it is likely that there is significant horizontal heat transport by fluids flowing laterally in the sedimentary section.

Significant fluid flow through the seafloor is highly localized. Discharge is limited to a few areas where there is active venting of high-temperature water. The high-temperature vent field at Site 858 is located over volcanic edifices that were formed by extrusive volcanism in Middle Valley. The structure of seamounts is likely to be more comparable to the extrusive carapace characteristic of the upper crust at unsedimented ridges, and consequently may have a higher permeability in the vertical direction than the more pervasive sill-and-sediment sequence. Thus, these structures may serve as vertical conduits that bring high temperature fluids close to the seafloor and focus flow in the plumes that feed the vents.

ACKNOWLEDGMENTS

The Schlumberger logging on Leg 139 was carried out by J. Witkowski; much of the success of Leg 139 logging program is due to his efforts. J. Attryde and P. Esteves with SEDCO also provided essential help and advice. Special thanks are due P. Lysne of the Sandia Corporation, who loaned the Geophysical Research Corporation self-recording, high-temperature logging tool to the Ocean Drilling Program for Leg 139, and the JAPEX Corp., which loaned a wireline high-temperature tool that logs flow, temperature, and pressure. E. Scholz provided invaluable support in the extensive preparations for the cruise. This paper was greatly improved by the reviews of A. Fisher and E. Davis.

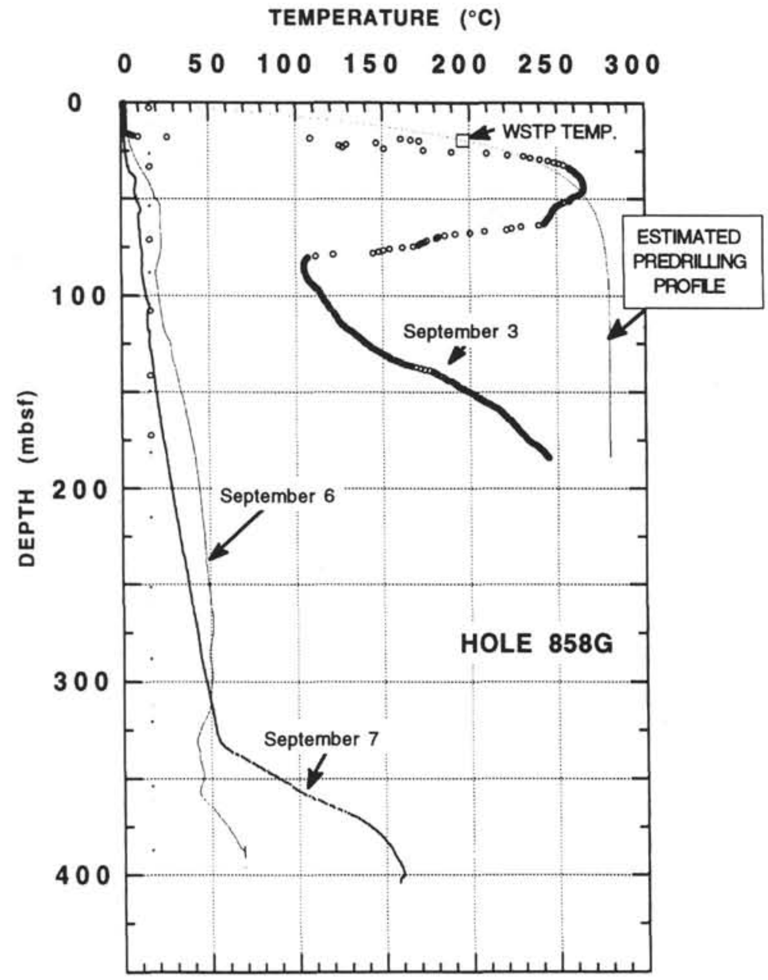

Figure 11. Subseafloor temperature measurements in Hole 858G. The open circles show a profile measured in the plugged casing. The other two measurements were made after the hole was drilled to total depth. The low gradient in the upper 330 m of these profiles indicates flow of water down the hole; the break in gradient at 330 m on the September 7 profile indicates where water begins to flow into the igneous formations at that level. The WSTP measurement was made in nearby Hole 858B. The estimated profile that existed below the vent field prior to drilling is based on a one-dimensional model of upward advection at a rate of 40 cm – a^{-1}; i.e., $T(Z) = T_0 + (T_\infty - T_0)\exp(\beta \cdot Z)$, where $T_0 = 2.5$, $T_\infty = 280$, and $\beta = \frac{v\rho c}{k} = -0.062$.

REFERENCES*

Anderson, R.N., and Zoback, M.D., 1982. Permeability, underpressures, and convection in the oceanic crust near the Costa Rica Rift, eastern equatorial Pacific. *J. Geophys. Res.,* 87:2860–2868.

Baker, P.A., Stout, P.M., Kastner, M., and Elderfield, H., 1991. Large-scale lateral advection of seawater through oceanic crust in the central equatorial Pacific. *Earth Planet. Sci. Lett.,* 105:522–533.

Becker, K., 1989. Measurements of the permeability of the sheeted dikes in Hole 504B, ODP Leg 111. *In* Becker, K., Sakai, H., et al., *Proc. ODP, Sci. Results,* 111: College Station, TX (Ocean Drilling Program), 317–325.

Becker, K., Langseth, M.G., and Von Herzen, R.P., 1983. Deep crustal geothermal measurements, Hole 504B, Deep Sea Drilling Project Legs 69 and 70. *In* Cann, J.R., Langseth, M.G., Honnorez, J., Von Herzen, R.P., White, S.M., et al., *Init. Repts. DSDP,* 69: Washington (U.S. Govt. Printing Office), 223–236.

Curray, J.R., Moore, D.G., et al., 1982. *Init. Repts. DSDP,* 64 (Pts. 1 and 2): Washington (U.S. Govt. Printing Office).

Davis, E.E., and Lister, C.R.B., 1977. Heat flow measured over the Juan de Fuca Ridge: evidence for widespread hydrothermal circulation in a highly heat transportive crust. *J. Geophys. Res.,* 82:4845–4860.

Davis, E.E., Mottl, M.J., Fisher, A.T., et al., 1992. *Proc. ODP, Init. Repts.,* 139: College Station, TX (Ocean Drilling Program).

Davis, E.E., and Villinger, H., 1992. Tectonic and thermal structure of the Middle Valley sedimented rift, northern Juan de Fuca Ridge. *In* Davis, E.E., Mottl, M.J., Fisher, A.T., et al., *Proc. ODP, Init. Repts.,* 139: College Station, TX (Ocean Drilling Program), 9–41.

Fisher, A.T., Becker, K., Narasimhan, T.N., Langseth, M.G., and Mottl, M.J., 1990. Passive, off-axis convection through the southern flank of the Costa Rica rift. *J. Geophys. Res.,* 95:9343–9370.

Langseth, M.G., Becker, K., Von Herzen, R.P., and Schultheiss, P., 1992. Heat and fluid flux through the sediment on the western flank of the Mid-Atlantic Ridge: a hydrological study of North Pond. *Geophys. Res. Lett.,* 19:517–520.

Shipboard Scientific Party, 1992a. Site 857. *In* Davis, E.E., Mottl, M.J., Fisher, A.T., et al., *Proc. ODP, Init. Repts.,* 139: College Station, TX (Ocean Drilling Program), 283–429.

————, 1992b. Site 858. *In* Davis, E.E., Mottl, M.J., Fisher, A.T., et al., *Proc. ODP, Init. Repts.,* 139: College Station, TX (Ocean Drilling Program), 431–569.

Tamaki, K., Pisciotto, K., Allan, J., et al., 1990. *Proc. ODP, Init. Repts.,* 127: College Station, TX (Ocean Drilling Program).

* Abbreviations for names of organizations and publications in ODP reference lists follow the style given in *Chemical Abstracts Service Source Index* (published by American Chemical Society).

Date of initial receipt: 9 February 1993
Date of acceptance: 9 September 1993
Ms 139SR-256